Bull. Mater. Sci., Vol. 36, No. 4, August 2013, pp. 647–652. © Indian Academy of Sciences.

Impact of interfacial interactions on optical and ammonia sensing in zinc oxide/polyaniline structures

MANSI DHINGRA, LALIT KUMAR, SADHNA SHRIVASTAVA†, P SENTHIL KUMAR and S ANNAPOORNI*

Department of Physics and Astrophysics, University of Delhi, Delhi 110 007, India
†Department of Physics, Dyal Singh College, University of Delhi, Lodhi Road, New Delhi 110 003, India

MS received 22 December 2011; revised 20 March 2012

Abstract. **Zinc oxide/polyaniline (ZnO/PANI) hybrid structures have been investigated for their optical and gas sensing properties. ZnO nanoparticles, prepared by the sol–gel method, pressed in the form of pellets were used for gas sensing. The hybrid ZnO/PANI structure was obtained by the addition of PANI on the surface of ZnO. The UV–Vis absorption of the modified pellets show band edge at 363 nm corresponding to ZnO, while a change in the absorption peaks for PANI was observed. The possible interaction between Zn^{2+} of ZnO and NH-group of PANI was confirmed using Raman spectroscopy studies. The results reveal that the hybrid structures exhibit much higher sensitivity to NH_3 gas at room temperature than blank ZnO, which is sensitive to NH_3 gas at higher temperature. This enhancement has been attributed to the creation of active sites on the ZnO surface due to the presence of PANI.**

Keywords. **Zinc oxide; polyaniline; gas sensing; morphology.**

1. Introduction

Gas sensor devices commonly employing metal oxide semiconductors (MOS) are based on the change in conductivity during interaction with gas molecules. The sensitivity exhibits a strong dependence on the operating temperature of the sensor (Kohl 2001; Batzill 2006; Korotcenkov 2007). It is well established that the sensing performance of the sensors can be enhanced by modifications of the microstructure, introducing dopant or using small amount of noble metal catalyst, etc (Ge *et al* 2007). MOS, however, suffers from the intrinsic disadvantage of poor selectivity, since a large variety of gases can induce resistance change. On the other hand, conducting polymers such as polypyrrole (PPy), polyaniline (PANI), polythiophene (P3HT), polyindole (PIN), etc act as sensors with selective response to the gas species making them a versatile gas sensor material (Virji *et al* 2004; Lange *et al* 2008; Gonsalves *et al* 2010). Simple method of synthesis in the form of powder, solution and thin films combined with room temperature operation are some of the key advantages of these organic conducting materials. In this study, we focus on the preparation of organic–inorganic hybrids with unique physical and chemical properties making them capable of sensing low concentration of reactive gases at room temperature and also at higher temperatures (Suri *et al* 2002; Geng *et al* 2007; Joshi *et al* 2008).

Zinc oxide, which is a wide bandgap semiconductor of *n*-type nature, has been chosen as the inorganic component, while proton-doped polyaniline has been selected as the organic counterpart. ZnO nanostructures such as nanofibres and nanorods have attracted the attention of several researchers for their potential applications as solar cells, gas sensors, biosensors, etc (Suchea *et al* 2006; Krunks *et al* 2008; Singh *et al* 2011). Solid-state method is commonly employed for synthesizing oxide powder, but shows difficulty in fine particle distribution because of abnormal grain growth at high temperature. Sol–gel method is preferred for synthesis of ZnO nanoparticles because of its chief merits, such as low processing temperature and uniform particle distribution (Niedererger 2007). Among conducting polymers, PANI stands out due to its unique electrical properties along with the flexibility of casting it in different forms; making it an ideal candidate for device applications. PANI is a potential *p*-type semiconducting material for use in electronic and opto-electronic devices such as light-emitting diodes, electromagnetic radiation shielding, gas sensor and biosensor (Ramanathan *et al* 1994; Chen *et al* 1996; Huang *et al* 2003; Bhadra *et al* 2008).

Hybrid structures can be obtained by *in situ* polymerization of the monomer in the presence of an oxide, or by a simultaneous gelation polymerization process or formation of interfaces in the form of films (Sharma *et al* 2006). The sensing behaviour depends not only on the individual organic/inorganic components, but also on the nature of interface between organic and inorganic components. Dhawale *et al* (2010) used an interface of polyaniline and ZnO, and reported an increase in sensitivity to LPG. In the present study, surface activation of ZnO nanoparticles by PANI has been carried out and an enhancement in ammonia sensing of ZnO/PANI hybrid structures by electrical method

*Author for correspondence (annapoorni@physics.du.ac.in, annapoornis@yahoo.co.in)

is reported. The enhancement is attributed to a strong interaction between ZnO and PANI at the interface and this is supported by optical studies.

2. Experimental

2.1 *Synthesis of zinc oxide nanoparticles*

ZnO nanoparticles were synthesized using sol–gel technique (Zhang *et al* 2007). Zinc acetate dihydrate [$(CH_3COO)_2Zn{\cdot}2H_2O$] as precursor and methanol as a solvent were used in the preparation. 0·6 M solution was mixed thoroughly using a magnetic stirrer maintaining the temperature at 60 °C for 2 h. The clear transparent solution thus obtained was poured in a round bottom flask and heated at 80 °C (higher than the boiling point of methanol) to evaporate the remnant methanol till a white powder (precursor complex) was formed. Thermogravimetric analysis of this white powder was done in order to find out the degradation temperature of acetates and other organic compounds so that it can be further heat-treated to obtain zinc oxide powder. The powder was then heated at 500 °C for 1 h in air to get ZnO nanoparticles. A portion of the powder (500 mg) obtained was compressed in the form of pellets by applying a pressure of 100 MP. Pellets of 1·2 cm in diameter and 1 mm in thickness were prepared using a hydraulic press.

2.2 *Synthesis of PANI and ZnO/PANI interfaces*

Polyaniline was synthesized by oxidative polymerization of aniline in the presence of hydrochloric acid using ammonium persulphate as an oxidizing agent. Monomer of 0·1 M aniline was dispersed in 1 M aqueous HCl in a double-walled flask, maintaining the temperature at 0–5 °C. Aqueous solution (1 M) of ammonium persulphate was added dropwise in the double-walled flask while stirring for 5 h. The solution obtained was filtered to remove the unreacted solution. The residue was washed 2–3 times with distilled water and then dried at 60 °C. This was followed by refluxing in methanol for 12 h to remove the oligomers. The residue was dried at room temperature and ground to get doped polyaniline powder (MacDiarmid 2001). In order to form an interface ZnO/PANI, PANI was dispersed in *N*-methyl pyrrolidone (NMP). PANI dispersion was prepared by dispersing 80 mg of PANI in 2 ml of NMP, which was sonicated to obtain a uniform dispersion. ZnO/PANI hybrid interfaces were prepared by dipping ZnO pellets in PANI dispersion for different time intervals viz. 2, 4 and 6 h. The pellets were then dried in ambient atmosphere.

2.3 *Characterization*

X-ray diffraction (XRD) analysis was carried out with a Bruker D8 diffractometer using CuKα radiation of wavelength, $\lambda = 1{\cdot}54056$ Å, for confirming the phase formation of ZnO, PANI and the hybrid system. Transmission electron microscope (TEM) image of ZnO nanoparticles was obtained using TECNAI G^2 20, 300 kV. Morphological investigations of ZnO, PANI and nanocomposites were carried out using scanning electron microscopy (SEM) (Zeiss, EVO) and their optical properties were studied using EVOLUTION 300 UV–VIS (Thermo Scientific) spectrophotometer. Raman spectra were obtained using Renishaw Invia Raman spectrometer, equipped with an argon ion laser (excitation wavelength, 514·5 nm). Gas-sensing studies were conducted by measuring the change in resistance of pellets exposed to NH_3 gas. The resistance was measured using a Keithley 2001 digital multimeter and current–voltage (I–V) characteristics were recorded using Keithley 2400 source meter.

3. Results and discussion

3.1 *Structural analysis*

Figure 1 shows XRD patterns of PANI, ZnO and ZnO/PANI hybrid interface (pellet dipped for 6 h in PANI dispersion). Figure 1(a) shows XRD pattern of PANI with a broad hump, suggesting an amorphous structure which is the characteristic of polyaniline (Lee *et al* 2008). Figure 1(b) clearly reveals polycrystalline nature and hexagonal structure of ZnO nanoparticles. The peaks were found to be matching with standard JCPDS value of ZnO. Figure 1(c) is the XRD pattern of ZnO/PANI interface which shows all the characteristic peaks of ZnO and a very small peak at $2\theta = 24°$, giving a probable signature of PANI.

3.2 *Morphological studies*

Figure 2(a) shows TEM image of ZnO nanoparticles annealed at 500 °C, with the corresponding selected area

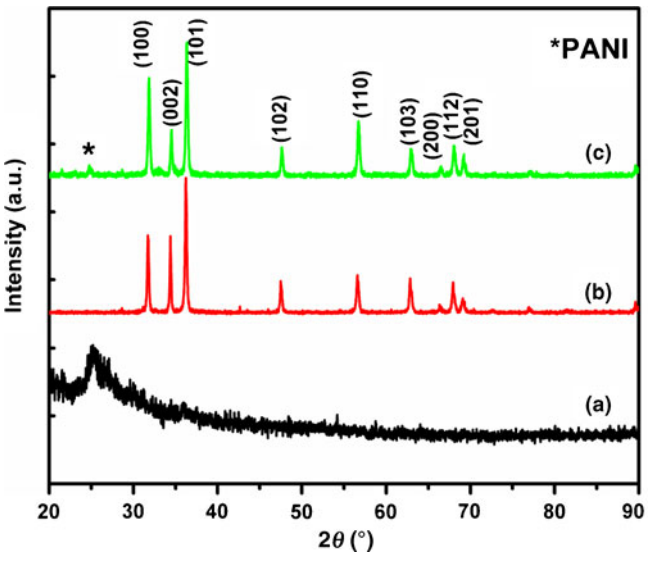

Figure 1. XRD patterns of (**a**) PANI, (**b**) ZnO and (**c**) ZnO/PANI hybrid interface.

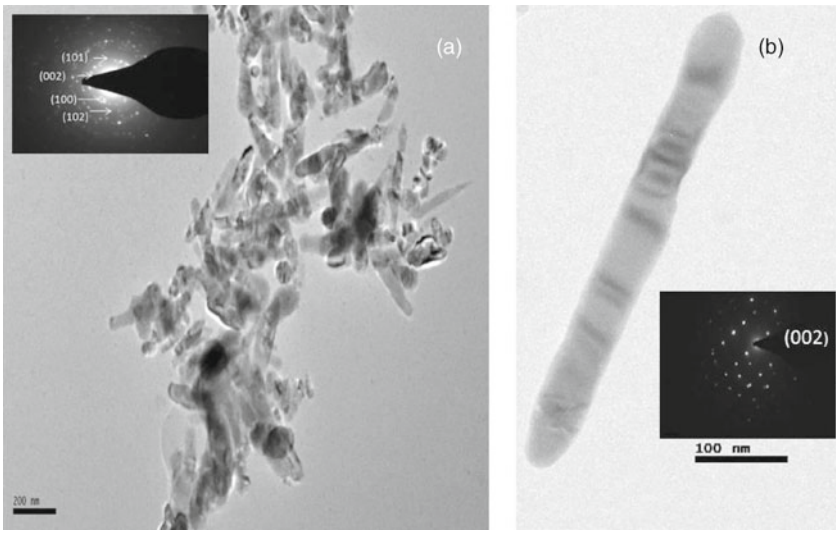

Figure 2. (**a**) TEM image with inset showing SAED pattern of ZnO nanorods and (**b**) TEM of single ZnO nanorod with inset showing SAED pattern.

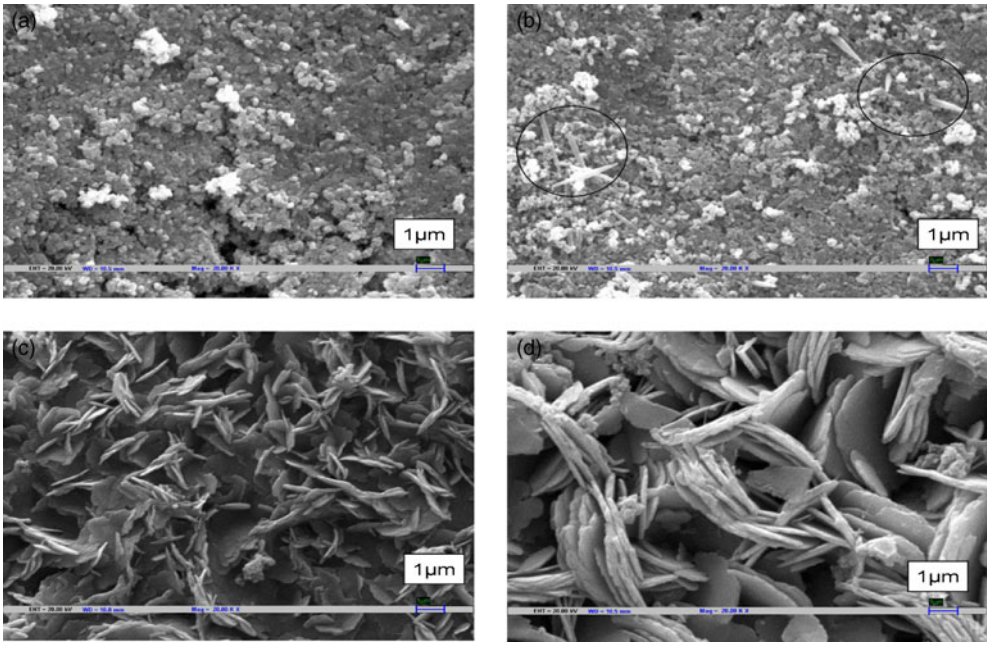

Figure 3. SEM image of (**a**) blank ZnO pellet and ZnO pellet dipped in PANI dispersion for (**b**) 2 h, (**c**) 4 h and (**d**) 6 h.

electron diffraction (SAED), respectively. SAED pattern of the nanoparticles confirms polycrystalline nature of the obtained nanoparticles. Figure 2(b) shows rod with the corresponding SAED, showing growth along the "*c*" axis.

The pellets were dipped in PANI solution for 2, 4 and 6 h and SEM of the surface is shown in figure 3. The blank ZnO pellet exhibits granular structures (figure 3(a)). Dipping ZnO pellets in PANI for 2 h shows a gradual formation of needle-like structure (figure 3(b)), which on further dipping for another 2 h act as nucleating sites resulting in layered structures or flakes (shown in figure 3(c)). A flake-like structure grows on dipping for 6 h in PANI (shown in figure 3(d)). The presence of polyaniline thus introduces a morphological change on the surface of ZnO pellets. Kang *et al* (2008) reported the self-assembly of semiconducting nanorods when placed in organic solution. The nature of interface so formed between ZnO and PANI can be visualized as adsorption of organic entities on the oxide base, giving rise to a change in morphology of the host matrix. This dynamic transition from rod-like to flake-like morphology is the manifestation of the physico-chemical interactions which occur due to variation in interfacial energy between the inorganic nanoparticles and organic dispersion. However, the exact mechanism of growth and corresponding

kinetics of the formation of such structures is not clear. The effect can be explained as a consequence of interfacial interactions between ZnO and PANI (Gupta *et al* 2006). Such flake-like growth was also found to occur on annealed ZnO, prepared by electrodeposition and chemical vapour deposition, at higher temperature (Zhang *et al* 2009; Singh *et al* 2010).

3.3 *Optical analysis*

UV–Visible spectroscopy was investigated to understand the optical behaviour of pristine ZnO pellet, ZnO/PANI interface and PANI dispersion. Optical absorption spectra for all the three are shown in figure 4. A clear band edge at 363 nm in figure 4(c) shows the characteristics of wurtzite hexagonal structure of ZnO (Kanade *et al* 2006). Figure 4(a) corresponding to doped form of PANI shows a peak at 330 nm which is due to the π–π^* transitions. The band at ~420 and ~850 nm refers to n–π^* and n–π transitions, respectively and signifies the formation of polarons, which depend on the amount of doping (Kulkarni *et al* 2004). Figure 4(b) of ZnO/PANI hybrid interface shows a band edge of ZnO at 363 nm and a peak at 445 nm and ~670 nm corresponding to PANI. However, shift in the position of the hump in ZnO/PANI interface (~670 nm from 850 nm) compared to PANI is because of the interactions between ZnO nanoparticles and PANI molecules. This implies that the nano-ZnO has an effect on doping level of conducting polyaniline (Ameen *et al* 2009). This indicates that the interaction is not a physical interaction.

3.4 *Raman analysis*

Presence of polyaniline in the hybrid was further confirmed by Raman studies. Figure 5 shows Raman spectra of PANI, ZnO and ZnO/PANI hybrid. Figure 5(c) shows E2 (high) mode at 437 cm^{-1} characteristic of wurtzite structure of ZnO (Lo and Huang 2010). Raman spectra of doped polyaniline in figure 5(a), has C–C stretching vibrations of benzene rings at 1628 cm^{-1}, C–N+ at 1331 cm^{-1}, C–N vibrations at 1252 cm^{-1}, C–H bending of benzene rings at 1192 cm^{-1} and NH bending at 1530 cm^{-1} reveals that polyaniline is in the form of emeraldine salt (Zhang *et al* 2005; Mazeikiene *et al* 2007; Jain and Annapoorni 2010). However, in Raman spectra of hybrid given in figure 5(b), the peak at 1530 cm^{-1} corresponding to the $^{-}$NH bending increases in intensity perhaps due to the linkages of imine units with ZnO. The presence of bands at 1584 cm^{-1} of C=C and at 1170 cm^{-1} of C–H bending of quinoids in the hybrid hint at the possible linkages between ZnO and PANI (Cochet *et al* 2000). However, a small peak at 437 cm^{-1} corresponding to ZnO appears in the hybrid maintaining its structure. Zheng *et al* (2002) proposed the interaction of $^{-}$NH group of polyaniline with Zn^{2+} ion of ZnO. So, the effect of interfacial interactions taking place between ZnO and PANI can be inferred from Raman spectroscopy also.

3.5 *Gas sensing analysis*

Gas sensing measurements were carried out on pellets of ZnO, PANI and ZnO/PANI hybrid using gold contacts (pellet dipped for 6 h in PANI dispersion) by two-probe method. Controlled quantity of NH_3 ~ 300 ppm was injected into the chamber. I–V characteristics were recorded for all the three pellets exposed to above ppm level and the characteristics are shown in figure 6. It is seen from figure 6(a) that pure ZnO showed linear behaviour with a very slight variation in current on exposure to NH_3, even up to 50 s. Pure PANI did show a marked variation in the current on exposure to NH_3 and its resistance increases sharply due to the deprotonation process of PANI (figure 6(b)). Deprotonation process reduces the PANI from emeraldine salt state to the emeraldine base state (Bavane *et al* 2010). The response curve for bare PANI pellet on exposure to 300 ppm of NH_3 is shown in

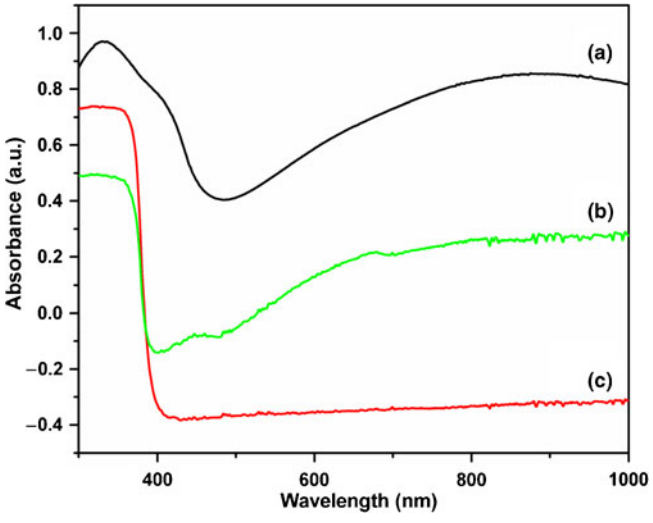

Figure 4. UV–Vis spectra (**a**) PANI, (**b**) ZnO/PANI and (**c**) ZnO.

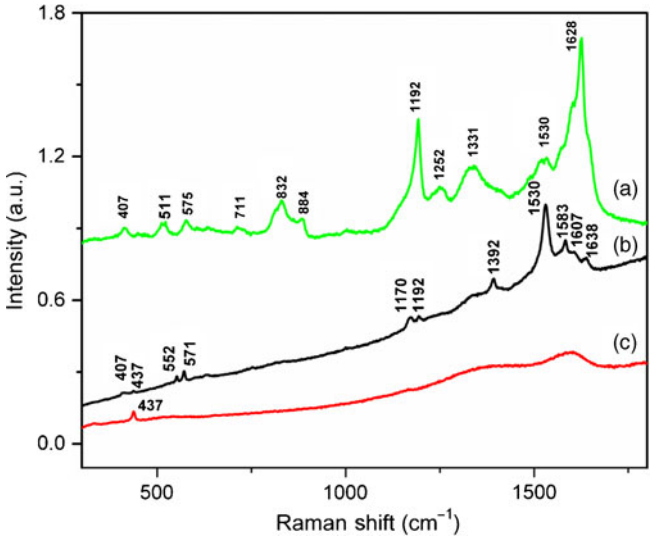

Figure 5. Raman spectra (**a**) PANI, (**b**) ZnO/PANI and (**c**) ZnO.

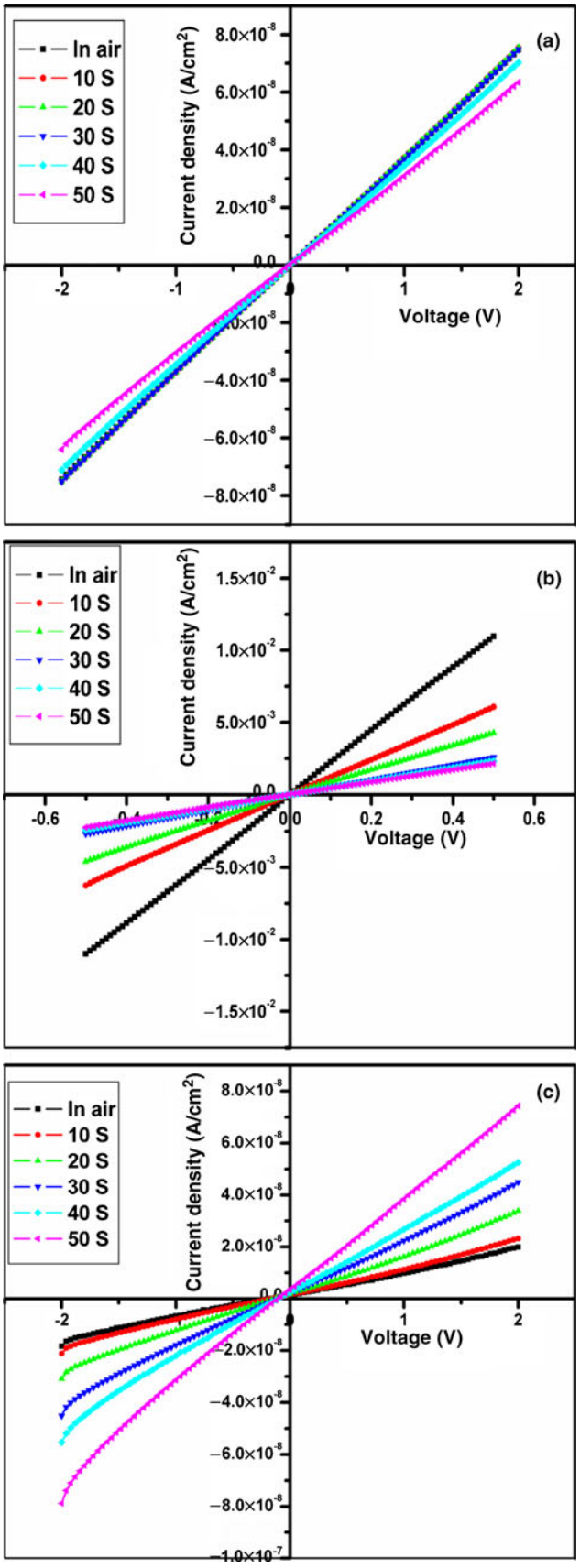

Figure 6. I–V characteristics of (**a**) ZnO, (**b**) PANI and (**c**) ZnO/PANI hybrid on exposure to 300 ppm NH_3.

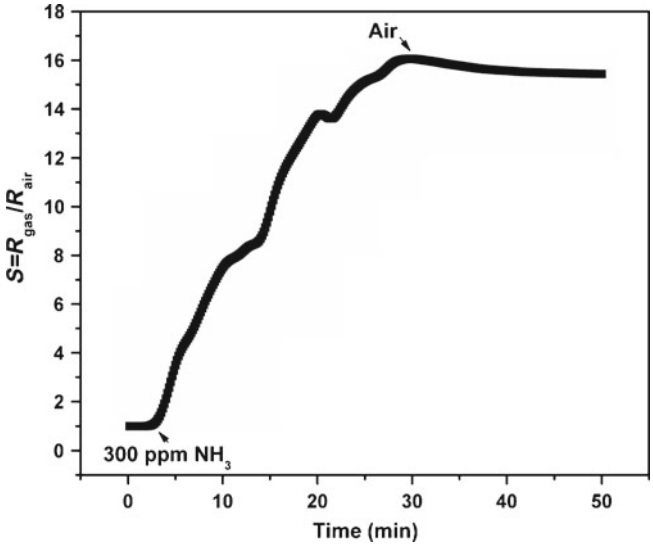

Figure 7. Response curve for blank PANI on exposure to 300 ppm of NH_3 at room temperature.

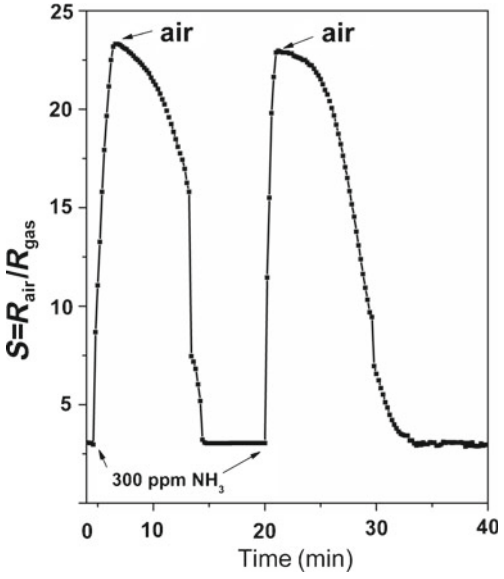

Figure 8. Response curve for ZnO/PANI hybrid on exposure to 300 ppm of NH_3 at room temperature.

figure 7. Although the sensitivity in this case is comparable to ZnO/PANI hybrid, very long response as well as recovery time makes the sensor unsuitable for practical applications.

The change in slope of I–V characteristics of ZnO/PANI hybrid on exposure to 300 ppm of NH_3 was large as compared to bare ZnO pellet shown in figure 6(c). This favourable performance of the hybrid gas sensor over the conventional ZnO gas sensor which performs amazingly well in detecting NH_3 at room temperature can be explained from the fact that PANI is a p-type semiconductor with holes as majority charge carriers. On the other hand, ZnO is a n-type semiconductor with electrons as majority charge carriers. The presence of polyaniline helps in absorption of NH_3 in the ZnO/PANI hybrid, hence giving a large variation in sensitivity as compared to blank ZnO and blank PANI. Therefore,

ZnO nanoparticles may act as a percolated high mobility pathway for electrons, PANI incorporation into oxide matrix creates an imbalance and a charge separation occurs at the polymer–nanoparticles interface. So, ZnO/PANI hybrid forms large number of *p–n* heterojunctions throughout the surface, giving rise to very high resistance at room temperature. When ZnO/PANI comes in contact with NH_3, this charge separation is released by NH_3 rupturing the heterojunctions and the resistance fall, down (Patil and Patil 2007). The depletion region that was created at the interface because of the difference in mobilities of semiconductor and polymer is broken and interparticle electron migration occurs through ZnO. In order to investigate the rate of change in resistance response behaviour of ZnO/PANI to 300 ppm of NH_3 was studied at room temperature and is shown in figure 8.

Response time was around 1 min, whereas recovery time was 16 min; this can be due to bulky nature of the sensor device (Kamble and Mathe 2008). This is due to the layered structure of interface as is evident from a SEM micrographs of the same (figure 3(d)). Absorption of NH_3 in this layered structure of sensing element makes the recovery time much longer than the response time.

4. Conclusions

ZnO/PANI hybrid interface was prepared by dipping ZnO pellets in PANI dispersion for several hours. Observation of the morphology reveals that the polyaniline affects the surface of ZnO. Interfacial interactions occurring between ZnO and PANI resulted in cohesion of PANI molecules with oxide matrix. Organic–inorganic hybrids so formed represent a new type of material which can be used as an electrical gas sensor working at room temperature. Although the recovery time of the hybrid gas sensor is quite long, hybrid gas sensor does not need to be heated during its operation. Organic entities that reside within the oxide base add functionality to it by changing its electrical and optical properties.

Acknowledgements

The authors would like to acknowledge the Textile Department, Indian Institute of Technology, Delhi, for providing the facility for recording SEM micrographs. They would like to thank University Science and Instrumentation Centre (USIC), University of Delhi, for XRD and TEM studies. One of the authors (SS) would like to thank the University Grant Commission for funding through the project F 32-23/2006 (SR).

References

Ameen S, Akhtar M S, Ansari S G, Yang O B and Shin H S 2009 *Superlatt. Microst.* **46** 872
Batzill M 2006 *Sensors* **6** 1345
Bavane R G, Shirsat M D and Mahajan A M 2010 *Sensors & Transducers* **113** 63
Bhadra S, Singh N K and Khastgir D 2008 *Polym. Eng. Sci.* **48** 995
Chen S A, Chuang K R, Chao C L and Lee H T 1996 *Synth. Met.* **82** 207
Cochet M, Louarn G, Quillard S, Buisson J P and Lefrant S 2000 *J. Raman Spectrosc.* **31** 1041
Dhawale D S, Dubai D P, More A M, Gujar T P and Lokhande C D 2010 *Sensor Actuator* **B147** 488
Ge C, Xie C and Cai S 2007 *Mater. Sci. Eng.* **B137** 53
Geng L, Zhao Y, Huang X, Wang S, Zhang S and Wu S 2007 *Sensor Actuator* **B120** 568
Gonsalves V C, Nunes B M, Balogh D T and Olivati C A 2010 *Phys. Status Solidi* **A207** 1756
Gupta S, Zhang Q, Emrick T and Russell T P 2006 *Nano Lett.* **6** 2066
He J, Zhang Q, Gupta S, Emrick T, Russell T P and Thyagarajan P 2007 *Small* **3** 1214
Huang J, Virji S, Weiller B H and Kaner R B 2003 *J. Am. Chem. Soc.* **125** 314
Jain M and Annapoorni S 2010 *Synth. Met.* **160** 1727
Joshi S S, Gujar T P, Shinde V R and Lokhande C D 2008 *Sensor Actuator* **B132** 349
Kamble R B and Mathe V L 2008 *Sensor Actuator* **B131** 205
Kanade K G, Kale B B, Aiyer R C and Das B K 2006 *Mater. Res. Bull.* **41** 590
Kang C C, Lai C W, Peng H C, Shyue J J and Chou P T 2008 *ACS Nano* **2** 750
Kohl D 2001 *J Phys. D: Appl. Phys.* **34** 125
Korotcenkov G 2007 *Mater. Sci. Eng.* **B139** 1
Krunks M, Katerski A, Dedova T, Acik I O and Mere A 2008 *Sol. Energ. Mater. Sol. C.* **92** 1016
Kulkarni M V, Viswanath A K, Marimuthu R and Seth T 2004 *Polym. Eng. Sci.* **44** 1676
Lange U, Roznyatovskaya1 V N and Mirsky V M 2008 *Anal. Chim. Acta* **614** 1
Lee K, Cho S, Park S, Heeger A J, Lee C W and Lee S H 2008 *Nature* **441** 651
Lo S and Huang D 2010 *Langmuir* **26** 6762
MacDiarmid A G 2001 *Rev. Mod. Phys.* **73** 701
Mazeikiene R, Tomkute V, Koudis Z, Niaura G and Malinaukas A 2007 *Vibr. Spectr.* **44** 201
Niedererger M 2007 *Acc. Chem. Res.* **40** 793
Patil D R and Patil L A 2007 *Sensor Actuator* **B123** 546
Ramanathan K, Annapoorni S and Malhotra B D 1994 *Sensor Actuator* **B21** 165
Sharma R, Suri K, Tandon R P, Lamba S and Annapoorni S 2006 *J. Appl. Phys.* **99** 023411
Singh N K, Jain B and Annapoorni S 2011 *Sensor Actuator* **B156** 383
Singh N K, Shrivastava S, Rath S and Annapoorni S 2010 *Appl. Surf. Sci.* **257** 1544
Suchea M, Christoulakis S, Moschovis K, Katsarakis N and Kiriakidis G 2006 *Thin Solid Films* **515** 551
Suri K, Annapoorni S, Sarkar A K and Tandon R P 2002 *Sensor Actuator* **B81** 277
Virji S, Jiaxing H J, Richard B, Kaner B R and Weiller H B 2004 *Nano Lett.* **4** 491
Zhang H, Chen G, Yang G, Zhang J and Lu X 2007 *J. Mater. Sci.: Mater. Electron.* **18** 381
Zhang N, Yi R, Shi R, Gao G, Chen G and Liu X 2009 *Mater. Lett.* **63** 496
Zhang J, Liu C and Shi G 2005 *J. Appl. Polym. Sci.* **96** 732
Zheng Z X, Xi Y Y, Dong P, Huang H G, Zhou J Z, Wu L L and Lin Z H 2002 *Phys. Chem. Commun.* **5** 63